Precision Assembly and Metrology of X-ray Foil Optics

Craig R. Forest[1], Matthew Spenko, Yanxia Sun, Michael McGuirk, Alexander H. Slocum, Mark L. Schattenburg
Massachusetts Institute of Technology, Cambridge, MA 02139

Keywords: x-ray telescopes, x-ray optics, Constellation-X, mirror alignment, precision assembly, MEMS, Shack-Hartmann, metrology, wavefront sensing

1 Introduction

Achieving arcsecond angular resolution in a grazing-incidence foil optic x-ray telescope such as the segmented mirror approach being considered for the NASA Constellation-X mission requires accurate and repeatable placement of thousands of individual foils. We are developing a method for assembling nested, segmented foil optics with sub-micron accuracy and repeatability using lithographically manufactured silicon alignment microstructures, called microcombs [1]. A system of assembly tooling incorporating the silicon microstructures, called an assembly truss, is used to position the foils that are then bonded to a spaceflight module. The advantage of this procedure is that the flight module has relaxed tolerance requirements while the precision assembly tooling can be reused. Previous work [5] has demonstrated that the microcombs can provide accurate and repeatable reference surfaces for the optic foils; current research has developed a device that makes progress towards actual flight module assembly. Key features include flexure bearings for frictionless motion of the microcombs, kinematic couplings to ensure repeatable alignment of successive flight modules, and flight module integration.

Metrology of the foil optics is critical to meeting the telescope performance goals. In addition to the sub-micron assembly tolerances, individual foils must be manufactured with figure error less than 500 nm over their 140×100 mm^2 surface area. A deep-UV Shack-Hartmann surface mapping tool has been created to determine whether the foils meet these manufacturing requirements and to provide active metrological feedback during the assembly procedure.

2 Design

2.1 Assembly truss

To accurately and repeatably assemble thin optic foils, an assembly truss has been designed and manufactured (Figure 1). In operation, optic foils are inserted into the device parallel to a reference flat. The foils' positions are constrained by two microcomb sets on the base and one microcomb set on the lid. Three flexure bearing assemblies, each containing a microcomb set (a spring microcomb and a reference microcomb), work in conjunction to position the optic foils. Figure 1 inset shows their design. To align the foils, a reference comb atop its flexure bearing is driven by a micrometer into contact with the polished reference flat, thereby aligning each of its "teeth." The spring comb is then actuated using a micrometer to force the optic foil into position against the reference comb's teeth. The flexure bearings provide hysteresis-free, friction-free support for reference combs to make contact with the reference flat and for the spring combs to impart forces to the foil.

The monolithic flexures have been manufactured from stress relieved aluminum 6061-T651 to prevent warping due to the release of internal stresses during manufacture. The four bar linkage design of the flexure bearings allows parallel motion between the top and bottom members. In fact, a parasitic pitch error in this motion is virtually eliminated with proper selection of the position of the driving point [6]. The flexures are actuated at half of their height by differential screw micrometers (Mitutoyo Model 110-102) which have a resolution of 0.1 μm. This resolution is necessary to achieve the microcomb placement accuracy of 1 μm. Force sensors (Honeywell, sold by Cooper Instruments Model LPM 560, LPM 562) are placed in between the micrometers and the flexure bearings to detect when contact with the reference flat occurs, since then the stiffness of the system changes. Before contact, the force per unit displacement is a function of the stiffness of the flexure bearings, force sensors, micrometers, and micrometer holders. After contact, there is

[1]email: cforest@mit.edu.

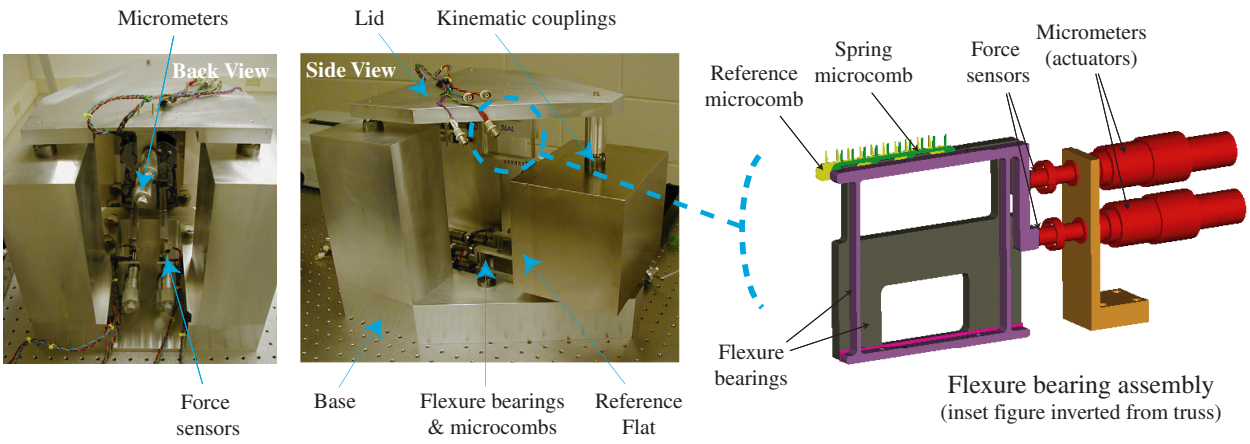

Figure 1: X-ray foil optic assembly truss. *Inset:* Flexure bearing assembly.

an additional stiffness component due to the Hertzian deformation of the microcomb. The force sensors are relatively insensitive to off-center plunger loading and have force ranges of 500 and 1500 grams-force for the reference and spring flexure bearings, respectively.

The structural parts of the assembly truss are stacked up with ball/v-block kinematic couplings at their interfaces. The ball and v-block design of these kinematic couplings theoretically allows repeatable assembly of the structure to less than 0.5 μm [2]. Fortunately, this error only impacts the foil assembly tolerances as a cosine term after flexure bearing actuation. The v-blocks are arranged such that the lines formed by the intersection of their respective faces intersect at the centroid of the triangle whose vertices are formed by the v-blocks themselves. This ensures uniform load distribution and prevents the faces from over-constraining the parts from misalignment.

The reference flat used as an alignment plane for the microcombs is a solid block of Aluminum 6061-T6 with 0.005 inches of electroless-plated nickel on its surface. The nickel is much harder than the aluminum to resist scratching during use. One face of the block is lapped and optically polished to 1 μm flatness peak-to-valley (P-V). Polished nickel was selected for a reference flat due to its low cost, hardness, and ease of machining.

A flight module containing the optic foils was incorporated into the design of the assembly tool. Prior to assembly, thirty foils are loosely held in this module by a set of "coarse combs." The entire structure is then loading into the precision assembly tool. The microcombs manipulate the foils into their aligned locations within the oversized slots of these coarse combs. Glue is then injected into holes on the coarse combs to secure the aligned foils in place. The flight module, containing the foils, is then removed and installed in the telescope. The flight module includes kinematic balls for the repeatable alignment with the base.

2.2 Shack-Hartmann surface metrology tool

The optical design for the deep-UV Shack Hartmann metrology tool is shown in Figure 2. The layout is similar to a Keplerian telescope design, where collimated input from the foil optic is demagnified to a collimated input to the wavefront sensor. This is accomplished using a large (200 mm diameter) off-axis parabolic mirror in conjunction with a relay lens. The magnification of the system and the advantage of this layout can be derived from the system matrix:

$$\begin{bmatrix} A & B \\ C & D \end{bmatrix} = \overbrace{\begin{bmatrix} 1 & 0 \\ L_2 & 1 \end{bmatrix}}^{\text{Propagation to } 2^{nd} \text{ lens from sensor}} \underbrace{\begin{bmatrix} 1 & -\frac{1}{f_2} \\ 0 & 1 \end{bmatrix}}_{\text{Refraction from } 2^{nd} \text{ lens}} \overbrace{\begin{bmatrix} 1 & 0 \\ f_1+f_2 & 1 \end{bmatrix}}^{\text{Propagation between lenses}} \underbrace{\begin{bmatrix} 1 & -\frac{1}{f_1} \\ 0 & 1 \end{bmatrix}}_{\text{Refraction from } 1^{st} \text{ lens}} \overbrace{\begin{bmatrix} 1 & 0 \\ L_1 & 1 \end{bmatrix}}^{\text{Propagation to } 1^{st} \text{ lens from foil}} = \begin{bmatrix} \frac{1}{M} & 0 \\ 0 & M \end{bmatrix} \quad (1)$$

where the 1^{st} lens is replaced by a parabolic mirror and the 2^{nd} is the relay lens. Choosing $L_1 = f_1 =$ 755.5 mm and$L_2 = f_2 =$ 75.0 mm, the system magnification M, given by matrix element D, reduces to

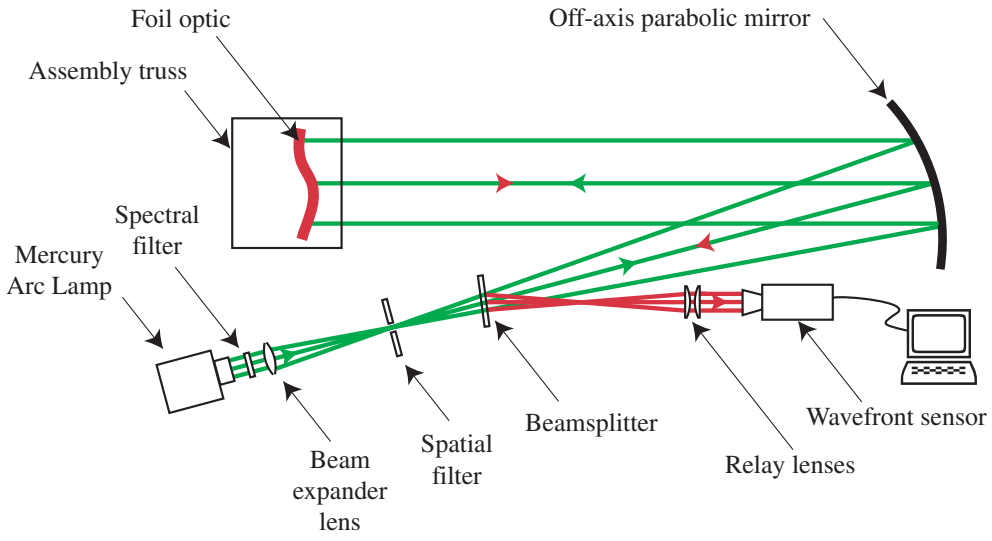

Figure 2: Shack-Hartmann metrology tool.

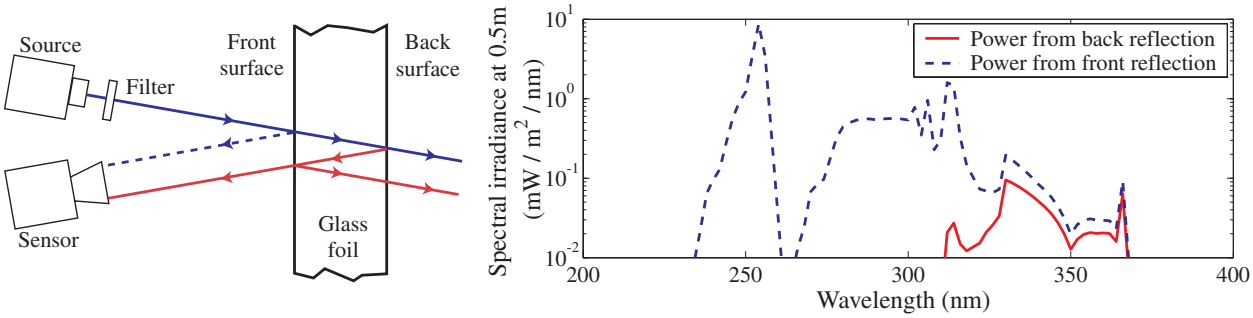

Figure 3: Irradiance from the glass sheets into wavefront sensor as a function of wavelength.

$-\frac{f_2}{f_1} = 0.1$. The system has no effective optical power as indicated by the B element. Element C shows that effective propagation distance is zero—the effects of diffraction are minimized at the image plane. The system matrix is diagonal, revealing that position and tilt are decoupled.

Deep-UV light is the most novel characteristic of the system. A 200 Watt broadband mercury arc lamp is spectrally filtered to allow mostly sub-visible wavelengths. Deep-UV light is exclusively required due to the optical transmission properties of the borosilicate glass foils (Schott, model D-263) proposed for the Constellation-X telescope optics. Light incident on the glass foil at wavelengths greater than 300 nm will partially transmit through the substrate and reflect off of its back surface. This will result in a doubled set of data on the wavefront sensor which will corrupt the wavefront reconstruction. The non-ideal spectral filter on the arc lamp does permit some longer wavelength radiation to reflect off of the foil optic, as shown in Figure 3. The theoretically computed irradiances take into consideration the spectral output of the arc lamp, the transmission curve of the spectral filter, and the optical properties of the glass to be tested. The ratio of the power into the camera from the front reflection to the back, calculated from the respective areas under the curves, is approximately 34.3. This back reflection power is below the sensor noise floor, making the error signal negligible. For comparison, if a higher wavelength HeNe laser were used for illumination, the ratio of the power from the front to back reflection would be 1.3. This would make the wavefront reconstruction erroneous.

A Shack-Hartmann [8] wavefront sensor (Wavefront Sciences, model CLAS-2D SMD) is used to image the optic under test. A key feature of this instrument is the lenslet array which dissects the incoming wavefront into 64×64 segments. Each of these segments is focused onto a detector located at the lenslet focal plane.

single slot repeatability test	displacement error, one σ (μm)			
	silicon wafer		fused silica plate	
	pitch	yaw	pitch	yaw
fixed lid and combs	0.26	0.39	0.59	0.23
dynamic lid, fixed combs	0.83	0.93	0.47	0.40
dynamic lid and combs	0.34	0.36	0.33	0.30

Table 1: Assembly truss slot alignment repeatability results.

The engineering tradeoffs with the performance of this instrument have been studied by Greivenkamp et al [4]. By comparing the focal spot locations on the detector with a reference surface to those from an aberrated surface, a difference map is calculated. Spatially integrating the slopes of this map allows the wavefront shape to be reconstructed. The instrument's sensitivity hinges on its ability to accurately centroid the focal spots. To do this, the focal spot should cover at least 10 pixels. The angular range of measurement involves the detector area allocated to each lenslet (area of interest or AOI). When the focal spot behind a lenslet appears near the edge of its AOI, crosstalk occurs and wavefront reconstruction is compromised, thereby limiting the angular range. The angular range for this camera can be estimated from the lenslet diameter of 0.224 mm and operating focal length of 17.904 mm to be approximately ± 6 mrad. The focal spot radius further reduces this range to ± 5.1 mrad. The sensitivity, a function of the pixel size, centroid estimation error, and focal length, can be calculated to be around ± 1 μrad. Over a 10 mm lateral distance in the magnified object plane, this corresponds to a theoretically measurable P-V height of ± 5 μm with a resolution of ± 1 nm. Previous surface mapping of stock silicon wafers indicate spatial distortion of this frequency and magnitude, so this instrument will be able to track subsequent flatness improvements from the original stock material.

3 Procedure and results

3.1 Assembly Truss

Numerous tests have been performed on the assembly truss to determine its ability to meet repeatability foil alignment goals of 1 μm. An autocollimator (Newport, model LAE500H) was used to measured the angular error of a foil located in a "slot," which was then converted to displacements. Previous experiments performed on a static breadboard test assembly system have demonstrated a 1 σ mounting slot repeatability error of about 0.11 μm in both axes [3]. This previous research defined repeatability as the standard deviation of a set of measurement collected by successively measuring, lifting, and replacing an optic foil against the reference microcomb teeth. This test was repeated with the new design and the data shows less than 0.05 μm for both pitch and yaw.

The current research involves a dynamic assembly truss, which strives to mimic the actual telescope foil alignment procedures. A static test was performed to obtain a baseline for repeatability. In this test, an optic foil was inserted into a slot, measured, then completely removed from the truss, reinserted, and remeasured. All mechanical parts on the truss were static. To test dynamic slot repeatability, two tests were performed. In the first test, the truss lid was removed and replaced as would be required for actual flight module assembly. The combs were not moved relative to the lid or base. The second dynamic test, which comes closest to actual flight module assembly, includes microcomb actuation to the planar reference flat in addition to lid reinstallation. These tests were conducted with both a 0.4 mm thick silicon wafer and a 3 mm thick fused silica plate coated with a reflective aluminum surface. Both materials were studied to understand the repercussions of thin foil deformation. Results from these tests are summarized in Table 1.

The results from the static test indicate that the repeatability of fully replacing an optic foil on the microcombs is approximately 0.3 μm in both axes. The second test includes the lid kinematic coupling repeatability error in addition. The final test effectively cancels out the kinematic coupling error by actuating the combs to the reference flat. Hence, in the final test, the optic foil placement repeatability appears to

dominate. Comparing the difference in results for the different foil thicknesses, thin foil deformation does not appear to be a significant contributor to the overall error.

3.2 Shack-Hartmann surface metrology tool

The surface metrology instrument has been successfully used to generate surface maps of large $\frac{\lambda}{30}$ reference flats, 0.45×100 mm diameter polished silicon wafers as commonly used in semiconductor industry, and 100×140×0.4 mm glass sheets. A sample image is shown in Figure 4.

The repeatability of the measurements has been primarily limited by random variations in the arc lamp caused by arc migration on the electrodes and convection currents inside the lamp [7]. Averaging 100 successive images has mitigated the effects of these variations, reducing the range of P-V surface maps to 5.0 nm (0.5 nm root-mean-squared (RMS)) over a minimum 100 mm diameter object size while the setup is unchanged. To determine the repeatability of the instrument for a human-in-the-loop environment, specimens were measured, physically removed from the metrology station, replaced and remeasured. Both the reference surface and the silicon wafer specimens were studied; results were similar. Repeatability measurements ranged 35.6 nm P-V with a 13.2 nm standard deviation. RMS surface variations ranged 14.0 nm with a 5.1 nm standard deviation.

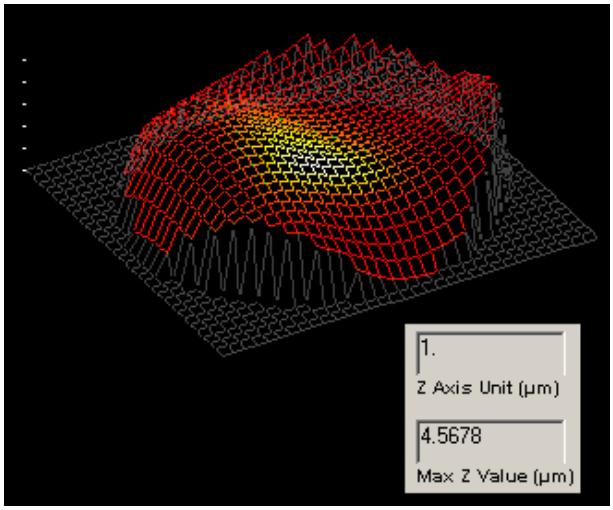

Figure 4: Reconstructed wavefront equivalent to a surface map at the object plane.

The accuracy of the system is difficult to quantify since aberrations in the lenses will contribute different angular errors to measurements at different spatial locations. To roughly estimate the overall accuracy of the system, two flats with factory-provided interferograms were measured. These interferograms reveal non-flatnesses of 2.6 nm RMS and 4.9 nm RMS, respectively. Comparing the two flats with the Shack-Hartmann system shows an average RMS surface difference of 17.6 nm. Overlapping the interferograms, the RMS deviation can be estimated to be $\sqrt{2.6^2 + 4.9^2} = 5.5$ nm. The difference between the Shack-Hartmann and interferometric data provides a crude estimation of the accuracy of the tool. Assuming root-sum-squared (RSS) stacking of errors, a conservative estimate of the accuracy yields $\sqrt{17.6^2 - 5.5^2} = 16.7$ nm RMS. Many factors contribute to the difference between the interferograms and Shack-Hartmann measurements. The mirrors are subjected to different temperatures and mounting forces between the instruments. Additionally, the uncertainty in the interferometric measurements is estimated to be $\frac{\lambda}{50}$ P-V.

In operation, the user will make a reference image with a flat, then substitute the optic under test. Based on the above analysis, the test measurement will be accurate to ∼17 nm and repeatable to ∼5 nm, RMS.

Results from glass metrology show no indication of back reflections in the raw data. The array of focal spots is regular and the frequency of spots is as expected, one per AOI. Large warp in pre-figured stock glass sheets makes their entire surface unmeasurable. A sample of this raw data is shown in Figure 5. Subset regions of the figure have been successfully measured to the accuracy and repeatability previously described.

4 Conclusions

Using a precision assembly truss, slot repeatability has been studied in an environment which closely matches that of the actual telescope optics assembly. This work has demonstrated that the assembly technology can meet the 1 μm Constellation-X foil placement repeatability requirement. Future work will include study of the accuracy of the microcombs.

A Shack-Hartmann surface metrology tool has been developed that permits metrological feedback of optic foils under consideration for the Constellation-X mission. This feedback is crucial during the assembly procedure since gravity, friction, and other forces can distort the wafers beyond the assembly tolerance.

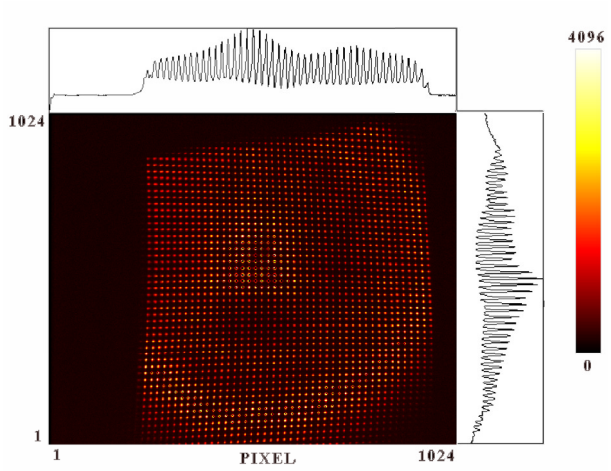

Figure 5: Raw data onto wavefront sensor from Schott D-263 glass sheet.

This instrument can be used to determine if a surface is meeting the current 500 nm global flatness manufacturing requirement. The surface mapping data is accurate to ∼17 nm and repeatable to ∼5 nm, RMS. Non-flat figures can also be studied up to a dynamic range of ± 250 μrad at the object plane. The 200 mm diameter viewing range can accommodate the proposed 140×100 mm^2 foil optic surface area.

5 Acknowledgments

We gratefully acknowledge the support of the students, staff, and facilities from the Space Nanotechnology Laboratory. This work is supported by NASA Grants NAG5-5271 and NCC5-633.

References

[1] C. G. Chen, R. K. Heilmann, P. T. Konkola, O. Mongrard, G. P. Monnelly, and M. L. Schattenburg. Microcomb design and fabrication for high accuracy optical assembly. *J. Vac. Sci. Technol. B*, 18:3272–3276, 2000.

[2] M. L. Culpepper, A. H. Slocum, and F. Z. Shaikh. Compliant kinematic couplings for use in manufacturing and assembly. In *International Mechanical Engineering Congress and Exposition*, Anaheim, CA, November 1998.

[3] Olivier Mongrard et al. High precision assembly and metrology of x-ray foil optics. In *Proc. Sixteenth Annual ASPE*, Crystal City, Virginia, November 2001.

[4] John E. Greivenkamp, Daniel G. Smith, Robert O. Gappinger, and Gregory A Williby. Optical testing using shack-hartmann wavefront sensors. In *Proc. SPIE*, number 4416, pages 260–263, Boston, 2001.

[5] Olivier Mongrard. High accuracy foil optics for x-ray astronomy. Master's project, Massachusetss Institute of Technology, Department of Aeronautics and Astronautics, September 2001.

[6] Yoichi Muranaka, Makato Inaba, Takeo Asano, and Eiichi Furukawa. Parasitic rotations in parallel spring movements. *Int. J. Japan Society of Precision Engineering*, 25(3), 1991.

[7] Oriel Instruments, http://www.oriel.com. *The Book of Photon Tools*, 2001.

[8] Ben C. Platt and Roland Shack. History and principles of shack-hartmann wavefront sensing. *Journal of Refractive Surgery*, 17:573–577, 2001.